

PROCESSING AND CHARACTERIZATION OF MICRO AND NANOCELLULOSE FIBRES PRODUCED BY A LAB VALLEY BEATER (LVB) AND A SUPER MASSCOLLOIDER (SMC)

IPSITA SAHOO,[§] PALLAVI GULIPALLI,[§] KAUSHIK CHIVUKULA and
RAMESH ADUSUMALLI

*Department of Chemical Engineering, Birla Institute of Technology and Science,
Pilani, Hyderabad Campus, Hyderabad, Telangana 500078, India*

✉ *Corresponding author: R. Adusumalli, ramesh.babu@hyderabad.bits-pilani.ac.in*

[§]*Authors contributed equally to this work*

Received February 20, 2023

Cellulose nanofibers, known for their high aspect ratio (>150), are difficult to process and characterize due to a variety of reasons, including lower diameters. In this work, cellulose micro and nanofibers produced by a Lab Valley Beater (LVB) and a Super Masscolloider (SMC) were characterized using optical microscopy and SEM. The thermal degradation behavior was analyzed using thermogravimetric analysis and solar radiation tests. With decreasing clearance between two grinders, SMC refining resulted in fibres with smaller diameter (400 nm to 8 µm) and a marginal increase in the number of fines was noted. LVB refining resulted in fibres with shorter length (500 µm), but a significant increase in the number of fines, contributing to higher tensile strength. The tensile strength of SMC sheets was 10-fold lower and severe ductile fracture was observed when compared to LVB refining. However, a 30 °C increase in thermal stability was found for fibres produced by SMC compared to LVB refining. This could be due to lesser heterogeneity in fibre morphology (reduced packing density), lack of surface fibrillation (reduced mechanical interlocking) and altered cellulose-lignin interaction for SMC refined fibres. Hence, it can be recommended to use blends of LVB and SMC refined fibres to make sheets for applications involving higher temperatures (250 °C) and higher tensile strengths (25 MPa), but the sheets need to be fabricated using the cast evaporation technique by maintaining the water bath temperature at 95-98 °C. The dust capturing ability of SMC sheets was tested using a dust sampler and it was found that sheet SMC_0.01 can capture PM_{2.5} dust particles, *i.e.* a weight increase of 7% was noticed in 6 h.

Keywords: mechanical refining, nanocellulose fibres, LVB, SMC, cast evaporation, PM_{2.5}

INTRODUCTION

Wood consists of cellulose (40-50%), hemicelluloses (25-30%) and lignin (25-35%), along with a small amount of extractives.^{1,2} Hemicellulose is the short chain, branched polymer that interacts with cellulose and lignin to strengthen cell walls. Lignin is the glue-like substance that binds cellulose fibres together and also imparts structural rigidity to the cell wall.³ Elementary fibrils, with a length of < 1 µm and diameter ranging from 1.5-3.5 nm constitute the basic structural unit of naturally occurring cellulose. An aggregate of these elementary fibrils gives rise to a microfibril (length of <2 µm and diameter ranging from 5-10 nm). Bundles of microfibrils constitute a microfibril bundle (length

of >2 µm and diameter greater than 15 nm), and a collection of microfibril bundles forms the cellulose fibre found in plants.¹ The length of wood fibres typically ranges between 1 and 3 mm, and widths – between 10 and 50 µm. They contain a central, hollow portion (lumen) and an outer cell wall (thickness of 1-5 µm), as shown in Figure 1. The separation of lignin and hemicelluloses from wood fibres carried out by means of chemical pulping^{4,5} results in pulp fibres that are rich in cellulose content.

The cellulose fibres can be deconstructed to various types of nanocellulose, which are defined based on their morphology, like cellulose nanofibrils, cellulose nanocrystals, also called

cellulose nanowhiskers.⁶⁻⁸ Cellulose nanofibers have gained tremendous attention in recent years due to their extraordinary properties, such as high modulus, high specific strength, high surface area, high aspect ratio, biodegradability, biocompatibility, non-toxicity and renewability.⁹⁻¹¹ Some of the applications of nanocellulose fibres are in the field of nanocomposites, biomedical engineering, separation membranes, flexible electronics and sensors.^{1,6,11-12} Nanocellulose fibres can also be used as an additive in conventional paper-making processes.¹

The properties of nanofibres can be affected by the degree of fibrillation.¹³ Different mechanical and chemical treatments are followed for producing micro and nanocellulose fibres. Mechanical treatment of pulp fibres is the most prevalent way of producing nanofibres, which results in changes in morphology, density and porosity.¹⁴ Mechanical treatments include high pressure homogenization,^{11,15,16} Lab Valley beating (LVB),^{10,11,17,18} cryocrushing,¹⁵ PFI milling,^{10,11,17} microfluidization,¹⁵ ultrasonic fibrillation,^{9,15,19} and ultrafine grinding using a Super Masscolloider (SMC).^{15-16,20-22}

LVB is mainly employed as a pre-treatment step before subjecting pulp to higher refining intensities. Spence *et al.* reduced the length of Kraft hardwood pulp fibres,²⁵ Haule *et al.* deconstructed cotton fabrics into pulp,²⁶ Zeng *et al.* disintegrated overnight-soaked (bleached kraft softwood) pulp fibres using an LVB,²⁷ and Kumar *et al.* utilized a chemical-refining method with an LVB to successfully obtain micro-nanofibrillated cellulose from bleached softwood pulp.²⁸

The grinding or refining process using an SMC is simple, cheap and is a one-step high yield method for the production of nanocellulose, as compared to other methods.^{29,30} The pressure in the grinding zone results in the longitudinal sectioning of the fibres, thereby nano- and micro-scale fibres are produced.^{29,31} The characteristics of the resultant material is highly affected by the time of operation and number of cycles.³² Vanzetto *et al.* obtained cellulose nanofibres with diameters lesser than 150 nm after subjecting textile waste samples to 6 hours of milling,³³ and Bandera *et al.* reported a diameter of less than 50 nm for microcrystalline cellulose refined by 12 passes through SMC.¹⁶ Some of the advantages of this refiner include the possibility of omitting any fibre-shortening pretreatment and the ability to set the clearance between the grinding stones slowly

to zero (lower clearances produce a greater number of nanofibres).¹

Though studies were carried out using LVB and SMC refining, respectively, no comparison was done between the existing LVB refining and SMC refining to the best of the authors' knowledge. A comparison of these two techniques is motivated by the fact that one of the grinders is stationary and the other one is rotating, and the clearance between the two grinders is less than the fibre diameter. Other techniques, such as electrospinning, will yield only nanocellulose fibres in comparison with SMC, which can produce both micro- and nano-cellulose fibres. Also, other methods can be more time-consuming and require solvents to dissolve the pulp. This study aims at comparing the morphological characteristics and thermal behavior of micro and nanocellulose fibres obtained at different refining intensities and durations by LVB and SMC. The tensile behavior of the sheets made from LVB and SMC refined pulps were also compared. Since dust needs to be separated from hot flue gases or sheets need to be used for food packaging applications, emphasis was given on thermal, morphological, mechanical properties of SMC and LVB sheets.

EXPERIMENTAL

Kraft cooking of wood chips

Wood from a 6 year old subabul (*Leucaena leucocephala*) tree was used to make sapwood chips of about 2 cm x 2 cm x 2.5 mm dimension, followed by drying at 103.5 °C for almost 10 hours before cooking. Wood chips were then put in an autoclave (MetaLab MSI-41) at 120 °C for one hour for better impregnation of chemicals in the subsequent cooking process, which was carried out using a rotary pulp digester (UEC, Saharanpur, India). The digester can rotate at 12 rpm, while facilitating the diffusion of cooking chemicals into the wood chips (Fig. 1). A wood to white liquor ratio of 1:4 was maintained and the cooking continued for 3 hours at 165 °C.² Then, the pulp and black liquor were removed from the digester, as shown in Figure 1. The pulp from the rotary digester was thoroughly washed with tap water to remove residual black liquor and other water-soluble impurities. The washed pulp, as shown in Figure 1, was dried in a vacuum oven at 103.5 °C to remove the bound moisture.

Refining of wood pulp using a Lab Valley Beater (LVB)

A Lab Valley Beater (LVB) uses cutting, impact, and compression as refining mechanisms to damage cell walls. It is important to collapse the lumen of pulp (Fig. 1c) and partially damage the single fibres or cells

using grinding or refining to make a sheet.⁴ The pulp slurry to be refined is poured into the pulp chest and the refining process takes place when the pulp slurry passes through the gap between the rotating beater roll and the stationary beater plate (Fig. 2). The beater roll and plate have metal protrusions that enable compression of cell walls and cutting of pulp fibres. The pulp refined using LVB results in an increased portion of fines, as it reduces the length of fibres multiple times.

100 g of oven-dried pulp was soaked in 6 liters of water overnight. The pulp was found to be swollen as a result of soaking, which could help improve fibre flexibility and facilitated easier refining. The pulp slurry was charged into the LVB with an additional 2 litres of water to avoid clogging while grinding. Refining took 40 min in total, with 5.5 kg weight at 600 rpm.²³ Samples were collected at 20 minutes intervals of refining for further analysis.

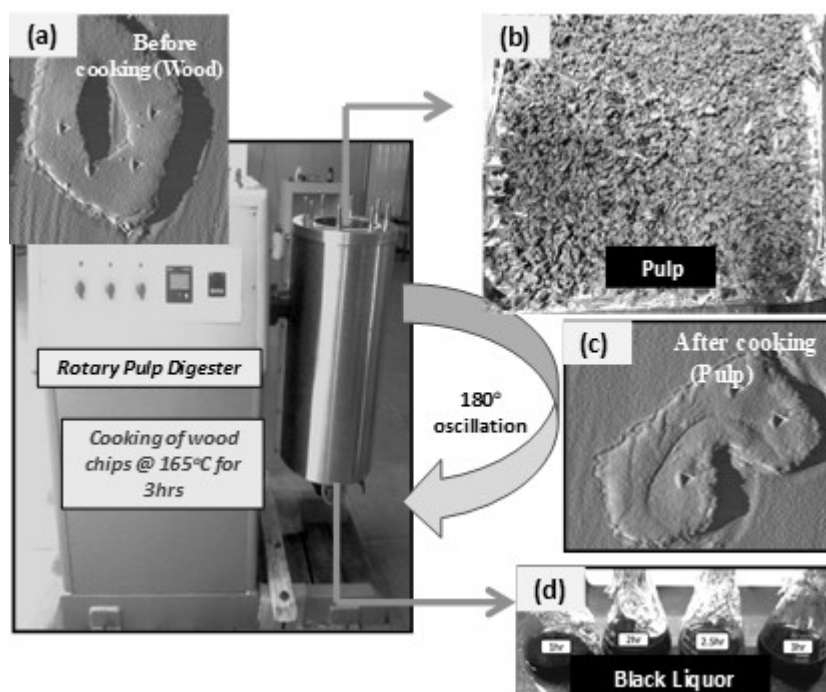


Figure 1: Rotary pulp digester with the lid open (rotation axis – horizontal on the plane of paper); (a) lumen and cell wall in wood fiber before cooking, (b) unbleached pulp after kraft cooking, with (c) collapsed lumen and damaged cell wall in pulp fiber; (d) black liquor

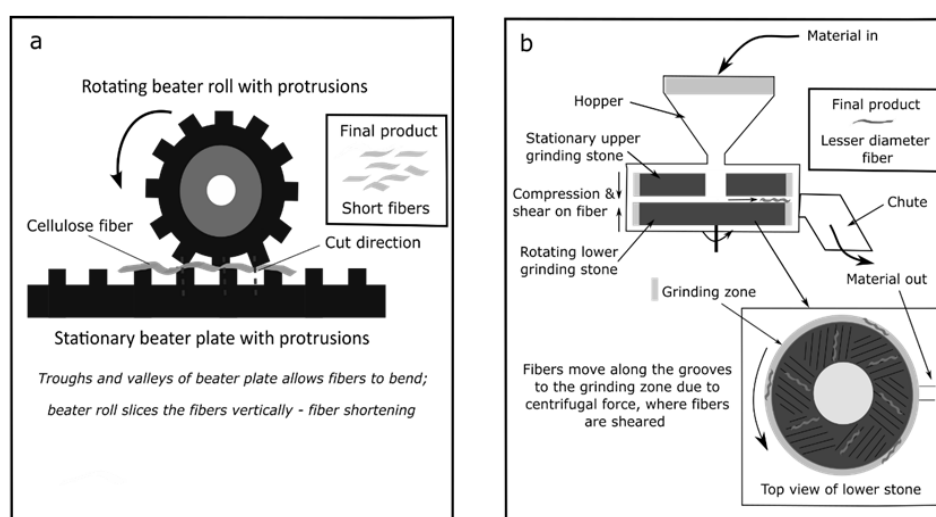


Figure 2: Schematic representation of refining mechanism of LVB (a) and SMC (b); Fiber cutting results in short length fibers in case of LVB (a) and fiber shearing/slicing in length direction results in short diameter fibers (b)

Super Masscolloider (SMC)

A Super Masscolloider (SMC) consists of two grinding stones made from SiC and Al₂O₃ powders bonded with a thermoset resin, making it non-porous and antibacterial. As shown in Figure 2, the upper stone is fixed in its position, while the lower stone is vertically adjustable and rotatable. The pulp slurry to be refined enters the SMC through the hopper after thorough mixing. The rotating bottom stone pushes the slurry to the edge of the grinding stones, *i.e.*, to the 17 mm grinding zone (as shown in Fig. 3), where refining takes place. The central part of both stones has symmetrical grooves and ridges, which enable uniform flow of the slurry. It is important to note that the pulp slurry will pass through these grooves at uniform speed due to centrifugal force induced by the clockwise rotation of the lower stone. The gap between the

grinding stones, which can be altered by turning the adjusting knob, can be set to zero in case of wet grinding, because liquid water acts as a continuous lubricant, thereby avoiding collision between the stones.²⁴ The refined slurry leaves the equipment easily through the chute, because the entire set-up is fixed to a concrete platform using anchor bolts with an inclination angle of 3°.

100 g of water-soaked pulp was refined using SMC at different dilution levels (14, 20 and 22 L of water for 0.4, 0.1 and 0.01 clearances, respectively). Initially, the pulp was refined using higher clearance (lower intensity) between the grinding stones to reduce the size of fibres gradually. As moving to lower clearance values (higher intensity) in the SMC, the viscosity of the slurry increased as a result of an increased number of micro- and nano-sized fibres, as shown in Table 1.

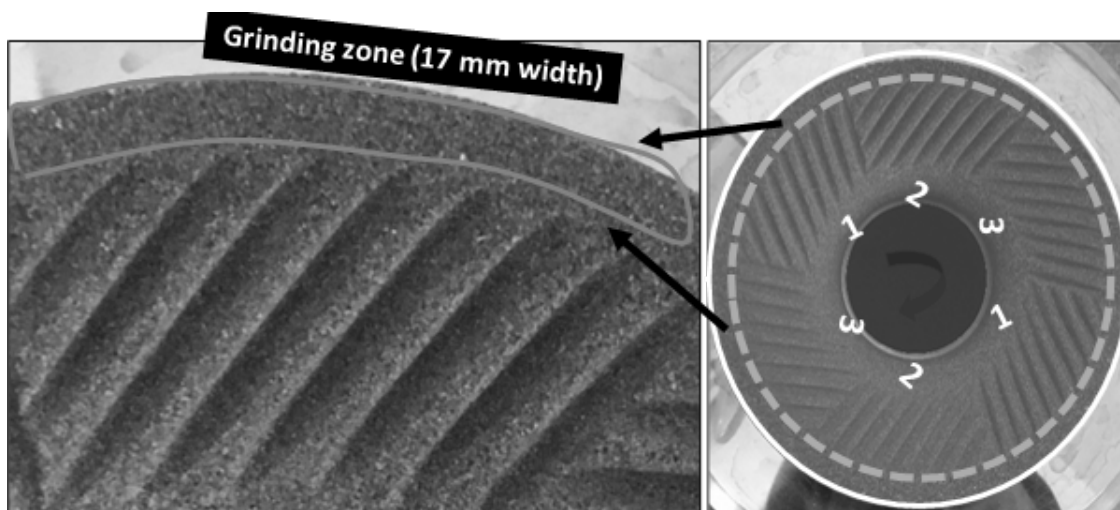


Figure 3: Super masscolloider (SMC) refiner; note the symmetry of the opposite set of grooves (1-1, 2-2, 3-3) in order to ease the uniform motion of slurry to the 17 mm grinding zone (gap between the outer solid circle and the inner dotted circle)

Table 1
Morphology of pulp microfibers after refining by LVB and SMC for different refining intensities (clearances) and durations

Refining technique (µm)	Refining time (min)	Average fiber length (µm)	Average fiber diameter	Fiber aspect ratio
LVB – 5.5 kg weight on lever	20	718 ± 267	20.1 ± 5.2	36
	40	559 ± 194	14.9 ± 4.0	38
SMC – 0.4 clearance	10	1126 ± 220	8.5 ± 2.6	132
	20	1100 ± 218	7.5 ± 1.9	147
SMC – 0.1 clearance	10	1069 ± 304	6.9 ± 1.8	155
	20	1066 ± 240	6.7 ± 2.4	159
	10	1000 ± 242	6.5 ± 2.6	154
SMC – 0.01 clearance	20	917 ± 242	5.1 ± 1.2	180
	40	901 ± 180	4.9 ± 1.1	184

For 20 min of refining time, the aspect ratio was found to be 147, 159 and 180 for SMC 0.4, SMC 0.1

and SMC 0.01, respectively.²³ Therefore, it was necessary to dilute the slurry¹⁶ to maintain a smooth

slurry flow through the grooves and avoid clogging of the lower grinding stone. The pulp was refined for a maximum of 40 min at each clearance, and samples were collected at 0.4, 0.1, and 0.01 (zero) clearance values and intervals of 10, 20, and 40 min for further analysis. Here, 0.01 indicates zero clearance (gap of less than 10 μm). The rpm was 1000 for 0.4 and 0.1 clearance values (low refining intensity) and 600 rpm for 0.01 clearance (high refining intensity). The objective of the SMC refining was to maintain the length and high aspect ratio of the fibres present in the slurry.

Characterization of LVB and SMC refined pulp fibres

The morphology of mechanically refined wood pulp fibres was analyzed using a stereo microscope (Olympus Corporation) and an optical microscope (Olympus SZ17), both in reflectance mode. Refined wet pulp suspensions were allowed to dry on glass slides and 60 fibres were considered for final measurements. To confirm the presence of nanofibres, a small amount of the slurry from SMC refining at 0.01 clearance (40 min) was poured on an indium tin oxide coated conductive glass slide and sputter-coated with 10 nm thick silver coating prior to SEM analysis. Refined and dried pulp fibres of 4.5-8.5 mg were taken into platinum pans for TGA analysis. A Shimadzu DTG60 machine was used with a heating rate of 10 $^{\circ}\text{C}/\text{min}$ between 33 $^{\circ}\text{C}$ and 600 $^{\circ}\text{C}$. Nitrogen gas was continuously purged with a flow rate of 100 mL/min till the pan temperature reached back to 30 $^{\circ}\text{C}$.

Processing of nonwoven sheets (cast evaporation)

Nonwoven sheets were fabricated from pulp slurry obtained from LVB and SMC refining by evaporating water, which resulted in an interconnected network of cellulose fibres. The sheets were formed using a water bath, wherein the consistency of the slurry and uniform distribution of heat were ensured throughout the silicone mould. 50 mL of pulp slurry obtained from LVB or SMC refining was poured into a silicone mould of dimensions approximately 6 x 3.5 x 3.5 cm^3 and was placed in the water bath at a temperature in the range of 95-98 $^{\circ}\text{C}$ until all the water was evaporated. Uniform nonwoven sheets were obtained within 6-7 h. However, densification using rollers was not carried out because retaining the fibrillated micro- and nanocellulose fibres on the "surface" is essential in capturing dust particles of $\text{PM}_{2.5}$ or having better interfacial bonding with polymer resins. Retaining nanocellulose fibres was not possible with the commonly used "mesh filtration", because nanocellulose fibres will pass through the square mesh of 120 μm length and it will be collected as a filtrate.

Characterization of nonwoven sheets

A nonwoven sheet fabricated from pulp refined at 0.01 clearance (40 min) was selected for cross-

sectional analysis using SEM. This analysis was aimed at observing nanofibres and the bonding characteristics of nano-cellulose and micro-cellulose fibres throughout the thickness of the sheet. For the preparation of the specimen, a 1 cm x 1 cm cross-section sheet was cut from the nonwoven sheet and embedded in a silicone mould using low viscosity Spurr epoxy resin, as described earlier.⁴ The cast was left to cure overnight in a vacuum oven at 60 $^{\circ}\text{C}$, followed by successive polishing with emery papers of decreasing roughness to expose the sheet's cross-section. Thereafter, the cast was subjected to microtoming or sectioning using a Leica RM2255 semi-automatic microtome. 10 μm thin sections were removed initially, followed by thinner sections of 5, 2, 1, and 0.5 μm to avoid surface cracks and minimize residual stresses. This sequential microtoming resulted in a smooth cross-section of the nonwoven mat for SEM analysis.

A texture analyzer (Stable Micro Systems, UK) was employed for tensile testing of nonwoven sheets made from LVB and SMC refined micro- and nanocellulose fibres.^{18,20} Rectangular samples of 0.3-1.8 mm thickness (variation is due to the absence of densification), length of 58 mm (gauge length of 25 mm), and width of 16 mm were loaded into the tensile set-up equipped with a load cell of 500 N and rubber-coated grips. Pre-test speed of 10 mm/min, test speed of 1 mm/min and a post-test speed of 10 mm/min were used as test parameters. Tests were performed at approximately 25 $^{\circ}\text{C}$ and 50% RH. Since unbleached sheets were considered in this study, a solar radiation test was carried out. A lamp with a power source of 150 W was used to simulate the solar spectrum, so that radiation on the sheet is around 1120 W/m^2 . Since there was difficulty in fixing the cast evaporation sheets (not densified), sheets made by vacuum filtration were used for this test. A test duration of 20 h of the diurnal cycle + 4 h light-off period was followed for 40 days. Air with 1.5 m/s velocity was circulated to achieve the ambient air temperature at the test item.

Dust sampling of SMC sheets

To evaluate the effectiveness of nanocellulose sheets for their dust capture capabilities, nonwoven sheets prepared from SMC 0.1 and SMC 0.01 refined fibers were placed in a dual channel dust sampler (Instrumex IPM-FDS 2510, India). This instrument uses a PM_{10} size separator, which traps particles with an aerodynamic diameter lower than 10 μm , followed by WINS impactor at downstream of PM_{10} size separator to filter out particles lower than 2.5 μm in diameter. In this study, nanocellulose sheets of 47 mm diameter, instead of glass nonwoven sheet (fibres of around 1 μm diameter), was locked into the WINS impactor holder using O-rings and tested with dust-laden air with the flow rate of 16.67 LPM for 6 hours. The sheet's weight change after dust sampling (which corresponds to $\text{PM}_{2.5}$ capture only) was used to gauge

the fine-dust capturing ability of these nanocellulose sheets. SMC_0.4 sheet was not considered due to high porosity (not reported here).

RESULTS AND DISCUSSION

Morphology of pulp fibres refined using the Lab Valley Beater (LVB) and the Super Masscolloider (SMC)

Table 1 summarizes the morphology of pulp fibres obtained after refining using LVB and SMC at different clearances and durations. Reduction in fibre length was reported (718–559 μm) in the case of LVB refining with increasing refining time (20–40 min). In the case of SMC refining, a reduction in fibre length was reported (1100–917 μm), considering the refining time of 20 min, and lowest and highest clearance. This result might be attributed to the presence of symmetric grooves and ridges on the grinding stones of SMC, which might have enabled the equipment to retain the length of pulp fibres (Figs. 2-3). This finding also corroborates the use of LVB as a mechanical pretreatment step to reduce the length of pulp

fibres, reducing the clogging difficulties in high pressure homogenization.²⁸

Stereo micrographs of LVB refined pulp (Fig. 4) revealed a larger proportion of fines when compared to SMC refined pulp (Fig. 5a). Cutting, shearing, and impact forces (Fig. 2a) in the LVB decreased the length of fibres and resulted in a greater number of fines. As shown in Figure 4, the number of fines increased with increasing refining time (20 min to 40 min). In the case of SMC refining, cutting is absent, which helps retain the length of fibres, thereby producing a smaller number of fines. As shown in Figure 5, the number of fines increased with decreasing clearance (0.4 to 0.01). It is evident from Table 1 that the length of LVB refined fibres (559 μm) is lower than that of the fibres refined with SMC (901 μm) in the case of 40 min of refining. SMC refining allowed retaining the length of original pulp fibres (almost 1.2 mm), thus amounting to a lesser decrease in length and a lower number of fines.

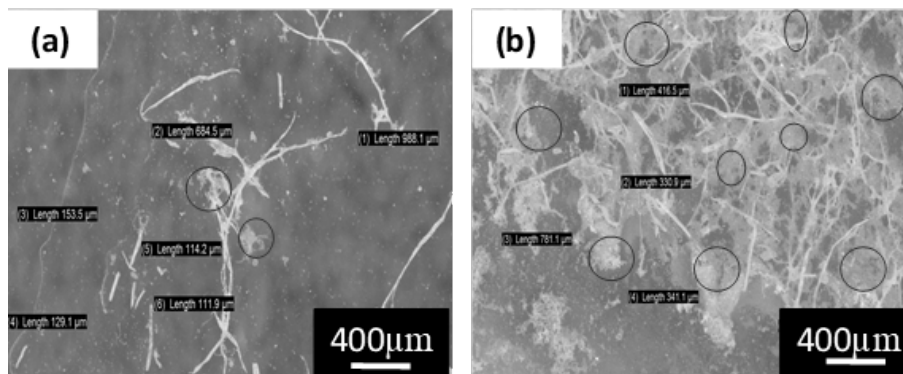


Figure 4: Microscopic images of LVB refined pulp fibers during (a) 20 min, (b) 40min (note the higher number of solid circles in (b), indicating more fines due to an increase in refining time)

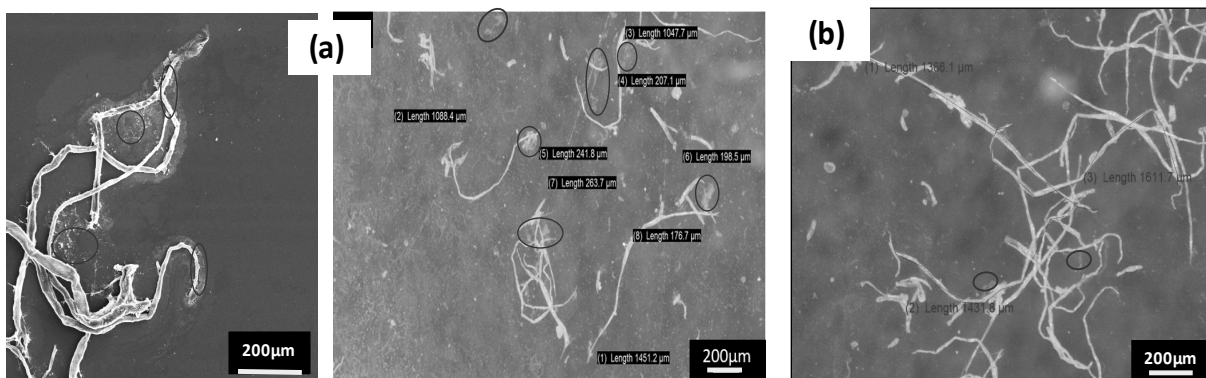


Figure 5: Microscopic images of micro- and nanocellulose fibers after refining in SMC at 0.01 clearance (a), and after refining in SMC at 0.4 clearance (b); note the greater number of fines (more circles) in (a) due to low clearance

However, refining using SMC led to a decrease in fibre diameter (4.9 μm), compared to

LVB refined pulp fibres (14.9 μm) in the case of 40 min of refining. This could be caused by

shearing and compression in longitudinal direction occurring in SMC refining. This is in contrast to the uneven surface of the beater plate, which allows fibre bending and thereafter fibre cutting/shortening in LVB refining (as explained schematically in Fig. 2).

Optical microscopy analysis revealed a sharp decrease in the diameter (20.1 μm to 14.9 μm) of pulp fibres with an increase in refining time (20 min to 40 min) in the case of LVB refining. However, SMC refining resulted in a gradual decrease in diameters with an increase in refining intensity and time, as shown in Table 1, with the value reaching around 5 μm for 0.01 clearance. The diameter of the pulp fibres did not change considerably after refining at 0.1 clearance in the SMC, even with increasing refining time. One possible explanation is that the progressive increase in dilution levels, while decreasing gap or clearance, might have resulted in lesser attrition among fibres and lower concentration of fibres in the grinding zone.

Refining using SMC yielded pulp fibres with higher aspect ratios reaching above 180, owing to its ability to retain the length of fibres during the refining process. An increasing trend in the aspect ratios of pulp fibres was observed with an increase in refining intensity and time, as shown in Table 1. When comparing between LVB and SMC, for 40 min of refining, the aspect ratio increased from 38 (LVB) to 184 (SMC 0.01), which indicates the use of SMC refining as a possible alternative to LVB refining to produce a blend of micro- and nanocellulose fibre-based sheets, which can serve as dust capturing filters or better reinforcement in polymer composites due to higher surface area. Considering their lower

length and lower aspect ratio, LVB refined fibres cannot be used as dust capturing filters because of high porosity, and could serve as “fillers only” in polymer composites.

Diameter measurement of nanocellulose fibres using SEM

SEM analysis was carried out to gauge the presence of micro- and nanocellulose fibres in the refined pulp slurry obtained at SMC_0.4, 0.1 and 0.01 clearance (Figs. 6 and 7) and in the sheet obtained from SMC_0.01 clearance (Fig. 8). Few microfibrils (4-12 μm in diameter) with a lot of kinks, twists, and partially collapsed lumen can be seen in Figures 6 and 7a. Refining the pulp at SMC-0.01 clearance (also called zero clearance) resulted in a few nanofibres, along with few microfibrils (Figs. 7-8), wherein the refining time of 10-40 min and 600 rpm were maintained, resulting in a higher surface area. The arrangement and angle of the grooves that facilitate shearing action and compression on the fibres are solely responsible for producing these nanofibres. Figure 7 depicts nanocellulose fibres refined using SMC at 0.01 clearance (refined for 40 min). Few locations in the pulp fibres reveal exposed lumen, indicating shearing of fibre in the length direction. Figure 7 (b-d) reveals nanofibres (200-946 nm in diameter). Figure 7b indicates partially refined nanocellulose fibre, with a lot of twists and exposed lumen. Figure 7 (c-d) indicates long or high aspect ratio nanocellulose fibres with diameters less than 400 nm and lacking fibrillation due to compression occurring at the grinding zone. However, slight fibrillation, with fibril diameters of 80-113 nm, was found for fibres shown in Figure 7a.

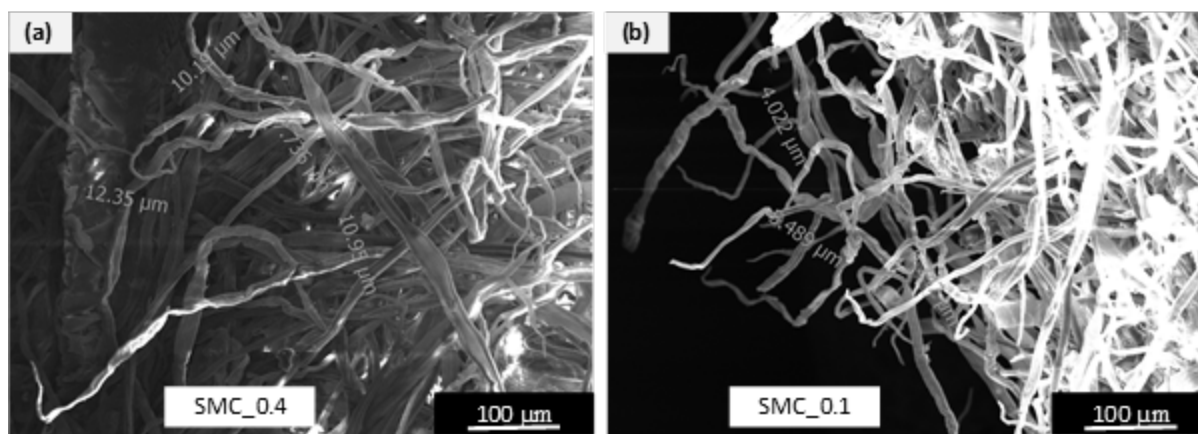


Figure 6: SEM images of micro/nanocellulose fiber network of SMC refined fibers; (a) clearance of 0.4, and (b) clearance of 0.1; note the reduction in fiber diameter with decreasing clearance from 0.4 to 0.1 (or increasing refining intensity)

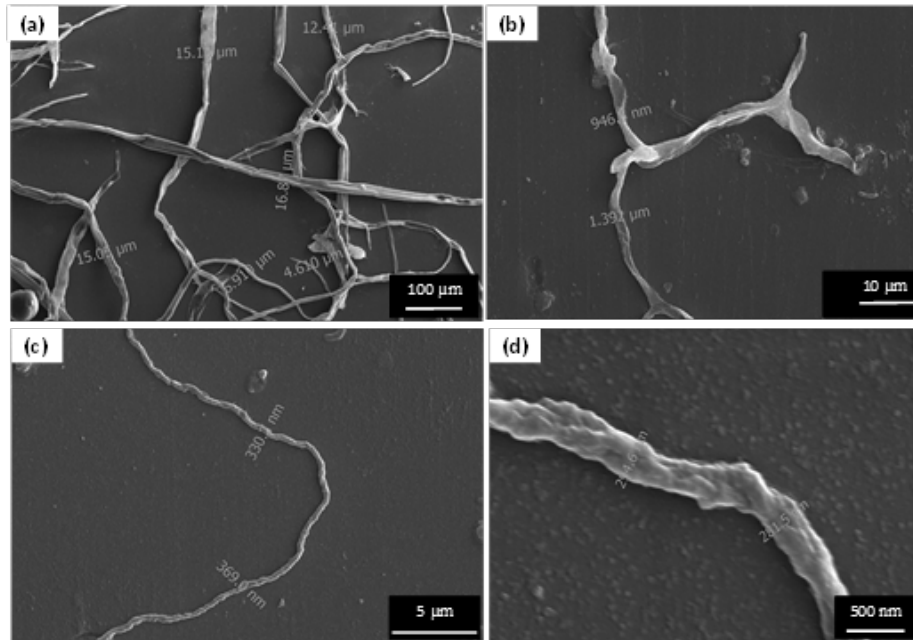


Figure 7: SEM images of nanocellulose fibers (refined pulp slurry of SMC 0.01, 40 min); clearance of 0.01 shows higher refining intensity than those of 0.1 and 0.4, which leads to a greater number of nanocellulose fibers

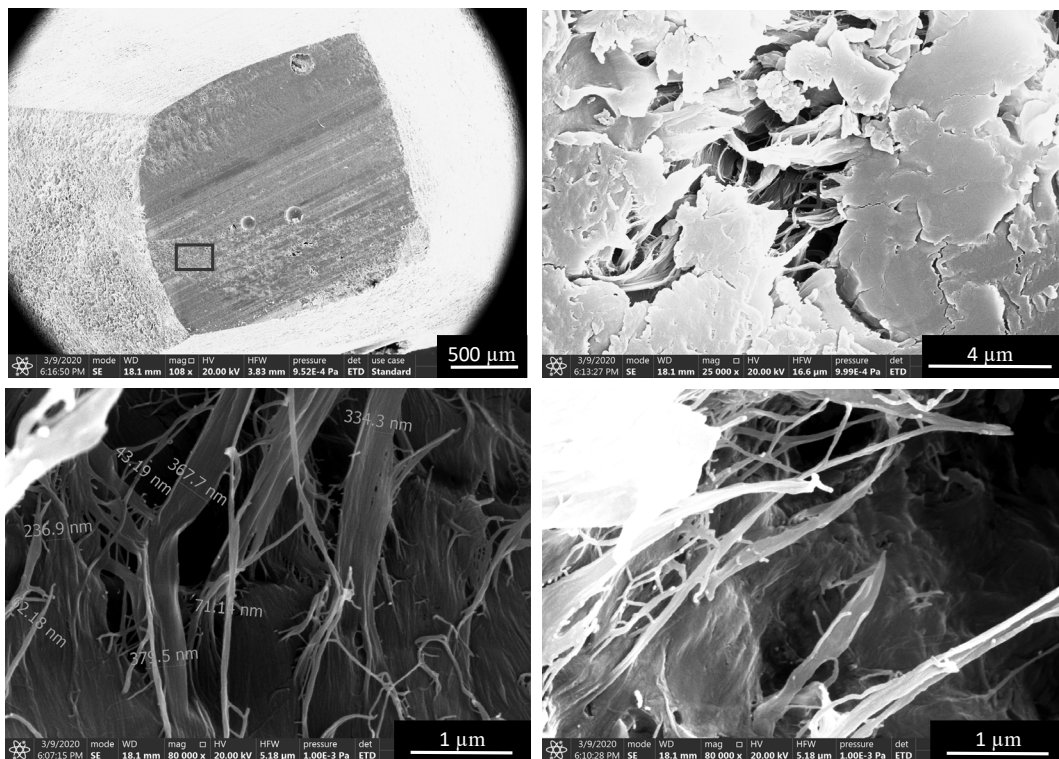


Figure 8: SEM images of nanocellulose fiber network

Figure 8 shows the smooth surface of the nonwoven sheet after sectioning using a microtome. The zone marked in the rectangle indicates the cross-section of SMC refined (0.01 clearance, 40 min) sheet embedded in epoxy resin. To confirm the presence of nanocellulose fibres obtained with this refining intensity, voids

in the sheet were imaged using SEM. It is interesting to note that nanocellulose fibres (40-400 nm in diameter) were entangled with each other, along with microcellulose fibres (as shown in Fig. 8). This observation indicates that sheet formation through cast evaporation allowed the retention of a higher number of nanocellulose

fibres generated during SMC refining. Lack of densification after forming the sheet, as discussed earlier, resulted in poorer networking (a lot of voids) of nano- and microcellulose fibres.⁴²

Tensile strength of micro- and nanocellulose sheets

Sheets made after LVB and SMC refining were tested for tensile strength. Stress-strain plots are shown in Figure 9, wherein the elastic region, plastic region, and fracture region can be seen. If 40 min of refining time is considered, the tensile strength of the sheets made from LVB refined pulp (46 MPa) was found to be higher than the sheets made from SMC_0.01 refined pulp (2.7 MPa). This might be attributed to the higher number of fines, leading to greater mechanical interlocking ability of LVB refined fibres (Fig. 4b). In the case of SMC, poor packing among fibres because of lack of densification and a lower number of fines led to decreased tensile strength (as shown in Fig. 9b). Because of this poor packing, the sheets made from SMC refined

micro- and nanocellulose fibres revealed severe ductile fracture, wherein maximum stress in the plot corresponds to crack initiation only (Fig. 9b). It confirms²³ that the tensile strength of sheets majorly depends on the fines content, as these sheets are nonwoven and not densified after processing. It is less dependent on fibre length, diameter, surface fibrillation and optimum cell wall damage, but this dependency of properties will vary with varying densification levels.

An increase in tensile strength (27–46 MPa) was observed with an increase in refining time in the case of LVB sheets (Fig. 9a). Longer refining time produced fibres with lesser diameters (Table 1) and damaged cell walls. This could result in better mechanical interlocking ability with other fibres, thus making their disentanglement difficult (as shown in Fig. 9a). Increasing refining time produced more fines (length of less than 200 μm) that would have filled the voids in the sheet, thereby increasing its tensile strength (fewer defects).

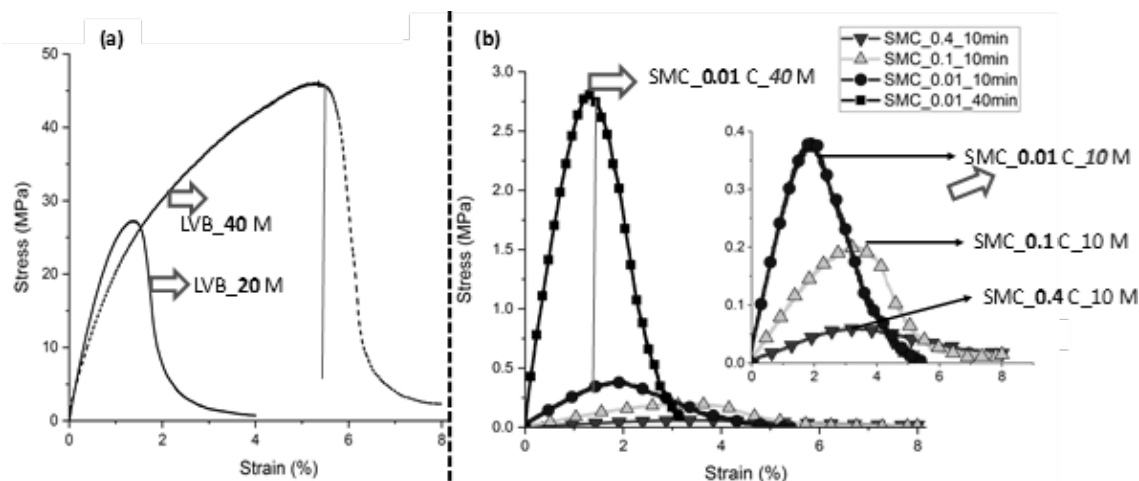


Figure 9: Tensile stress-strain plots of sheets made from LVB (a) and SMC (b) refined pulp fibers (0.4, 0.1 and 0.01 – clearance between stones, and 10, 20, 40 min – refining time)

The inset picture in Figure 9b indicates stiffer and stronger sheets with decreasing clearance (0.4–0.1–0.01). An increase in tensile strength (0.06 MPa, 0.20 MPa, 0.38 MPa) was observed with increase in refining intensity or decreasing clearance for SMC sheets in the case of 10 min refining (Fig. 9b). This could be due to a slight decrease in the length and diameter of pulp fibres, as shown in Table 1, and a slight increase in the fines content, as shown in Figure 5a. The strain corresponding to the onset of crack initiation decreases with decreasing clearance, indicating higher networking of fibres in the sheet, resulting

in higher modulus (not measured, but shown in Fig. 9b). As we move to 40 minutes of refining in SMC, a decrease in length (1000–901 μm) and diameter (6.5–4.9 μm), compared to 10 min refining, was noticed, as shown in Table 1. This reduction in length contributed significantly to increasing the fines content, which could contribute to better mechanical inter-locking between longer fibres, leading to better tensile strength, as shown in Figure 9b.

As shown in Table 2, pulp consistency also reduced with decreasing clearance (with an increase in refining intensity), which indicates an

increased number of fines contributing to higher tensile strength, as explained above. Pulp consistency is measured by taking the dry weight and wet weight of sheets processed using a 100 µm metallic mesh filter, which indicates that residual fibre length plays a critical role in consistency.²³ As a conclusion, the tensile strength of the sheet decreased with decreasing heterogeneity in fibre morphology, *i.e.* absence of fines in SMC sheets, which is in line with the use of LVB refining as strength enhancer due to a higher number of fines, as reported by Kumar *et al.*²⁸ Around 7.1% reduction in lignin content was reported by Wu *et al.*, when Aspen chips were subjected to prehydrolysis and mechanical refining by a juicer and PFI mill.³⁴ Therefore, it is recommended to wash the refined pulp and use ultrafine filters (alternative to the evaporation

technique) to make nonwoven sheets, wherein high tensile strength (due to retaining the fines) and hydrophilicity (due to reduction in lignin) are required.

Fractographic analysis was carried out on LVB_40 min and SMC_0.01_40 min sheets after tensile fracture (Figs. 10-11). From the fractographs of LVB sheets (Fig. 10a and c), it is evident that the fracture surface is “slightly” ductile and reveals higher fibre-fibre bonding strength (shorter fibres lead to a dense network). As explained earlier, a proper number of fines and a lot of surface fibrillation (dotted circle in Fig. 11c) induced excellent mechanical interlocking, thereby higher tensile strength (Fig. 9a). Crack initiation and propagation was very quick in the case of LVB sheets.

Table 2
Consistency of refined pulp slurries

Refining method	Consistency after refining
Before mechanical refining	18.3%
SMC – 0.4 clearance	15.7%
SMC – 0.1 clearance	14.9%
SMC – 0.01 clearance	11.4%

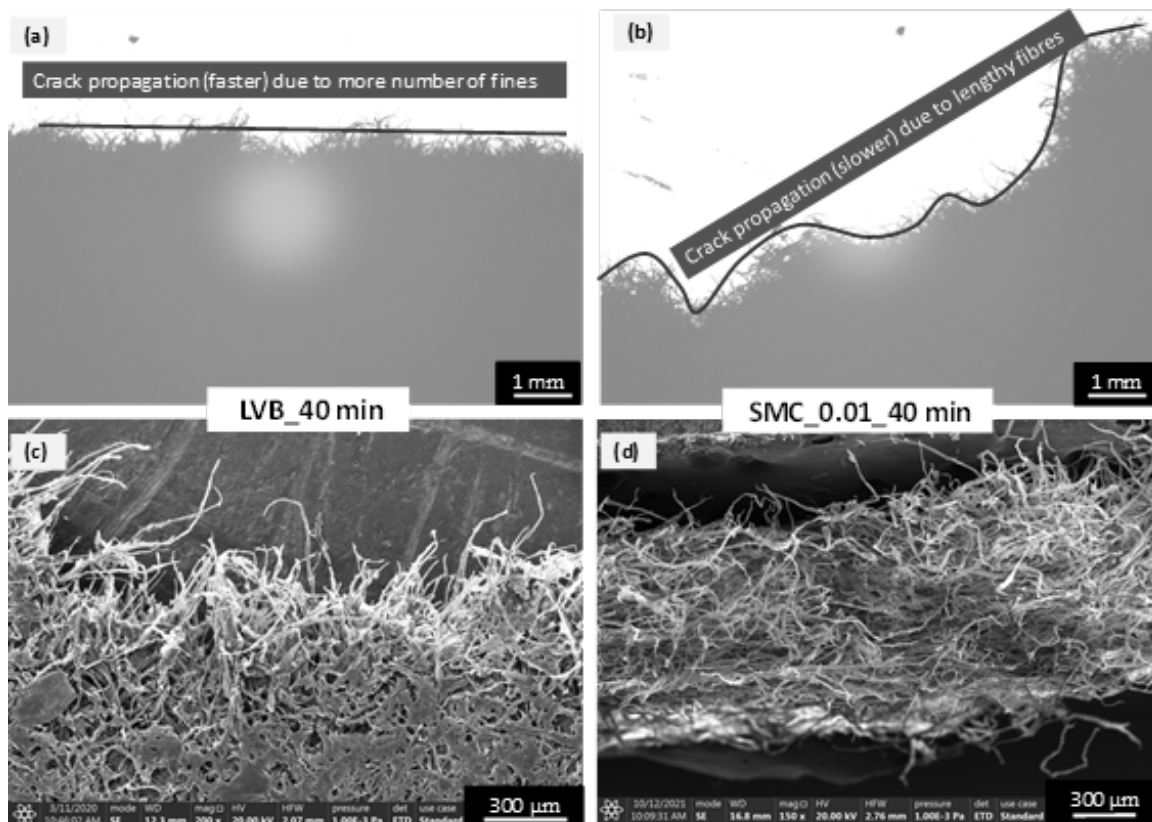


Figure 10: Tensile fractographs of LVB-40 min sheet (a and c) and SMC-0.01, 40 min sheet (b and d)

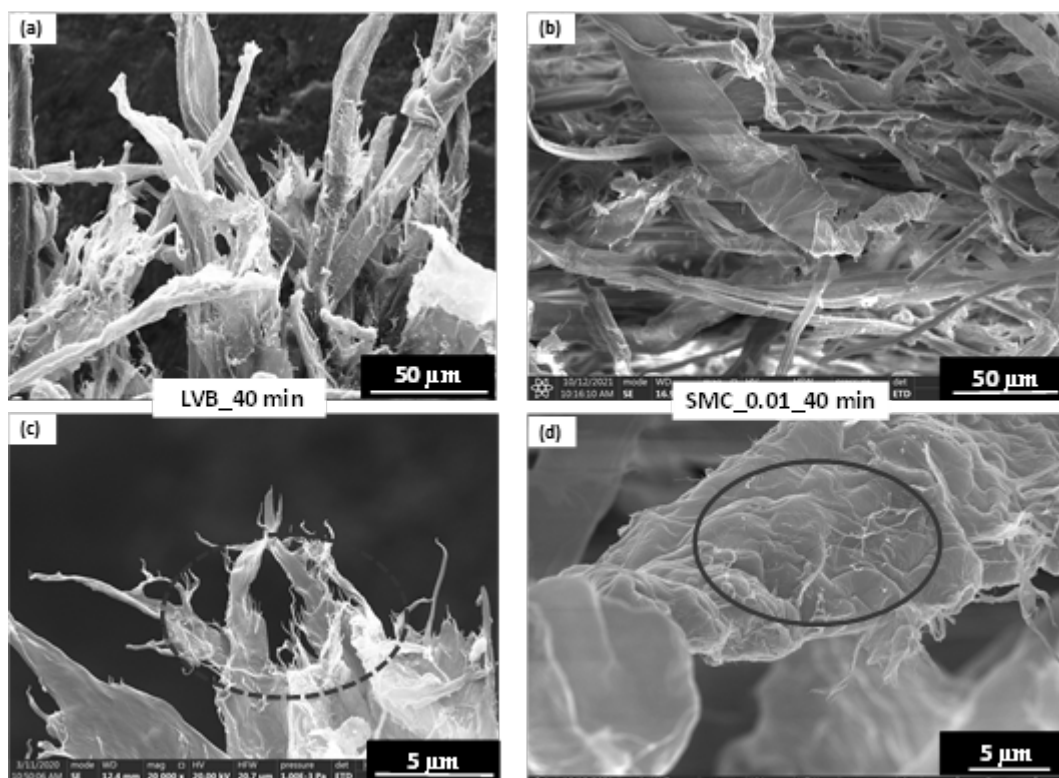


Figure 11: SEM tensile fractographs of LVB sheet (40 min) (a and c), wherein the dotted circle indicates severe fibrillation, and SMC sheet (0.01, 40 min) (b and d) wherein the solid circle indicates less fibrillation

From the fractographs of SMC sheets (Fig. 10b and d), it is evident that the fracture surface is “highly” ductile and characterized by shear fracture due to weak fibre-fibre bonding (longer fibres lead to a loose network). The angle of fracture is 30-40°, indicating shear and ductile fracture of the nonwoven sheet (Fig. 10b and d).¹⁸ Crack initiation started at one end and propagation was very slow due to lack of fines and lack of surface fibrillation. Upon applying load, loosely bound fibres are pulled out of the sheet, forming kink-like surfaces and a gradual decrease in fibre-fibre bond strength of the sheets leads to severe ductile failure. The gradual decrease in strength (post ultimate strength) is the indicator for the poorer network of the sheets (Fig. 11b). In SMC, smoothening of fibres happened due to extensive refining, resulting in loss of fibrillation (solid circle in Fig. 11d), contributing to poor mechanical interlocking of fibres in the sheet. A few zones of the fractured sheet indicate excessive shearing along the length, twists, kinks and fibre splitting (Fig. 11b). Figure 11d indicates slight fibrillation (on the side surface) and compression, contributing to lower tensile strength.

Thermogravimetric analysis (TGA) of micro- and nanocellulose fibres

Figure 12 depicts the thermal degradation behavior of refined fibres. The thermal degradation of LVB and SMC refined micro- and nanocellulose fibres showed almost similar behavior till 365 °C. The thermal degradation of cellulose samples can be divided into 3 zones. In zone I, a minor weight loss of the fibre sample occurs until the temperature of around 100 °C, after which, a plateau region starts and continues up to 220 °C. This decrease in weight is primarily caused by the evaporation of surface moisture from the fibres.

In zone II, which starts above 220 °C, a sharp decrease in the sample weight is observed and marks the onset of thermal degradation. At this temperature, the thermal degradation of cellulose, lignin and volatile components begins. The thermal stability of fibres slightly increased for SMC refined fibres, compared to LVB refined fibres, because the onset of degradation shifted from 249 to 273 °C at 10% weight loss, as shown in the inset picture of Figure 12. High refining intensity (decreasing clearance) in SMC causes an increase in surface area (reduction in diameters, as shown in Table 1) and a loose network of the

nonwoven sheet, due to a lower number of fines, which could have contributed to slightly better thermal stability. As the temperature increased in zone II, lignin and cellulose degradation started and depolymerization (endothermic reaction) of cellulose possibly occurred up to a temperature of 350-360 °C,³⁵ which contributed to a weight loss of ~67%, as shown in Figure 12.

In zone III, above 365 °C, there is a low weight loss of the sample, which is due to the existence of the cell wall composite structure,² inorganic components and extractives. The weight loss in this region was found to be proportional to the intensity of refining.

Excessive refining leads to severe cell wall damage, as shown in Figure 7b.²⁴ As refining intensity and duration is increased, the composite structure of the cell wall (dense network of lignin-cellulose) gets damaged, thereby resulting in a loose network of fibres. SMC_0.01 (40 min) refined fibres were found to have a looser network of fibres, compared to LVB (40 min)

refined fibres, as explained above. Previous studies in our laboratory have also shown that dense composite structure leads to higher residual mass.^{2,20} As shown in Figure 12, the residual mass at 600 °C was found to be 15.8%, 7.2%, 4.9% and 2.8% for LVB (40 min), SMC_0.4 (20 min), SMC_0.01 (20 min) and SMC_0.01 (40 min) respectively. With increasing refining intensity, *i.e.*, decreasing clearance in SMC and duration lead to a greater proportion of loose pulp fibres, thereby contributing to severe degradation in zone III. Chen *et al.* also reported lower residual weight for rice straw fibres with lower lignin content.³⁶

However, higher porosity in the nonwoven sheet (weak fibre-fibre bonding strength) in the case of SMC refined fibres led to an increase in thermal stability, but the residual mass at 600 °C was found to be low, *i.e.* 2.8%, because of the “damaged composite structure containing a higher number of nanocellulose fibres”.

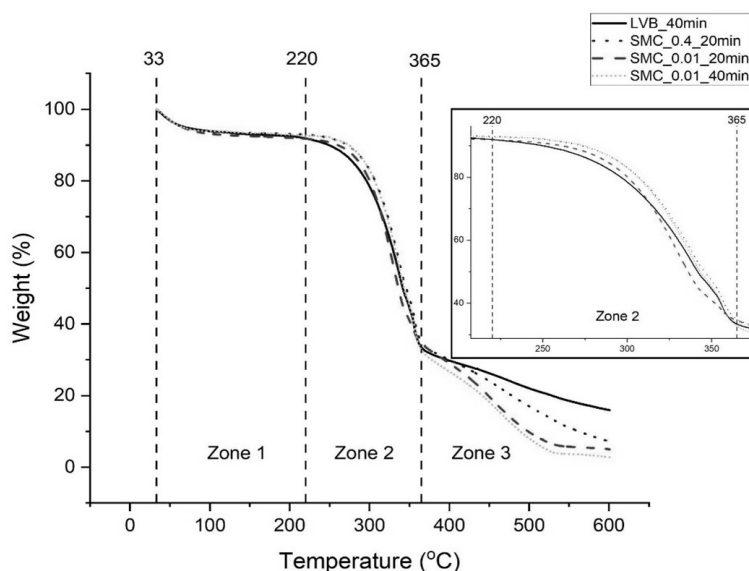


Figure 12: Thermogravimetric analysis of refined micro- and nanocellulose fibers (inset picture describes gradual degradation behaviour of Zone 2; 0.4 and 0.01 – clearance between stones, and 20, 40 min – refining time)

Solar radiation test of SMC refined sheets

Solar radiation tests for both SMC_0.1 and SMC_0.01 sheets (5 x 5 cm²) were carried out for 40 days, and no visible damage to the sheets was found, indicating the suitability of these sheets for outdoor applications. A surface temperature of 70 °C was measured on both sheets for the heat intensity of 1120 W/m² (1.1 sunlight). Optical microscopy images revealed no surface damage to micro/nanocellulose fibres, but SEM images

revealed shaded fibers (black color fibres), indicating the onset of degradation because of solar radiation, as shown in Figure 13. SMC_0.1 clearance sheets (average fiber diameter of 10 μm) present a higher number of pores, compared to SMC_0.01 clearance sheet (average fiber diameter of 4 μm), as shown in Figure 13. Since this test was carried out for 40 days, shading of fibres (changing from white to black color) was observed in a few areas, as shown (thick circles)

in Figure 13.² It is recommended not to use these micro/nanocellulose sheets continuously for 40

days above 60 °C.

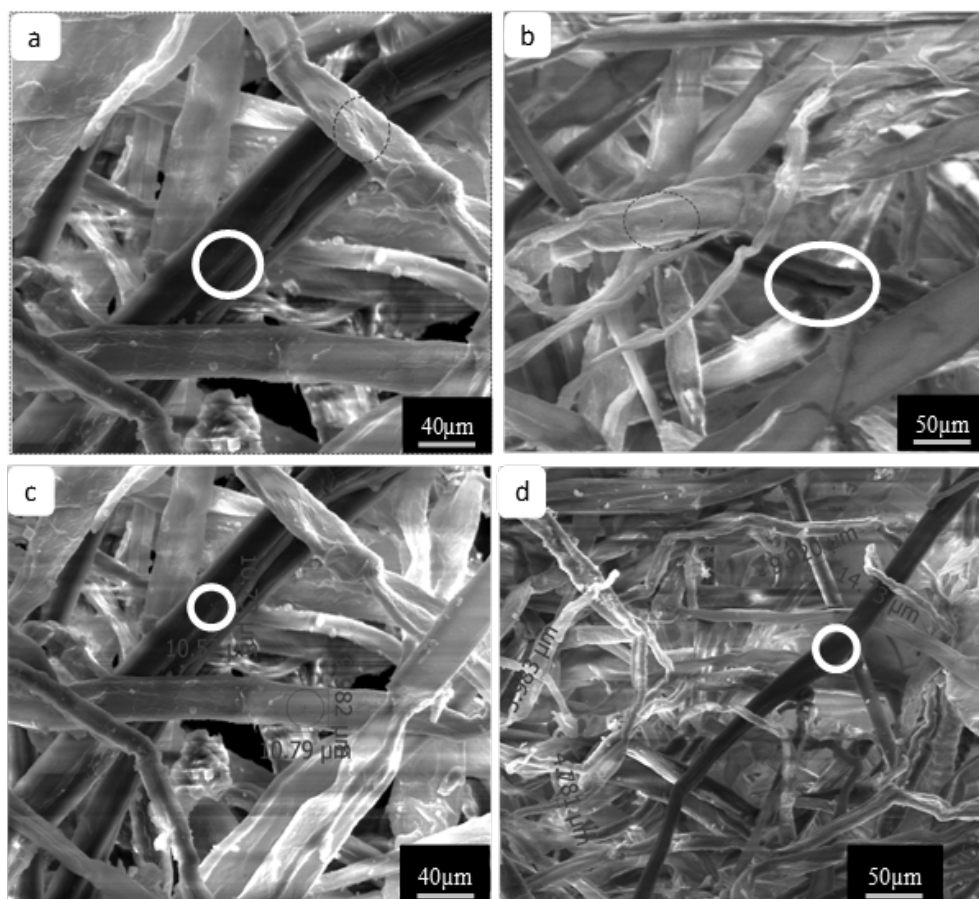


Figure 13: SEM images taken after 40 days of solar radiation test for (a and c) SMC_0.1 sheet, (b and d) SMC_0.01 sheet (thick solid circles indicate shaded (black colour) fibers, showing little degradation of cellulose fibers at 70 °C

Dust capture analysis of nanocellulose sheets

Particulate matter (PM) can be removed from dust-laden air using filters with high filtration efficiency, large filtration area, low pressure drops, and low regeneration frequency (frequency of removing clogged particles from the filter).^{37,38,43} Additionally, in order to have effective capture of dust by the filter medium, Lawrence and Liu³⁹ claimed that fibre diameters must be smaller. Therefore, these nanocellulose sheets have been envisaged as potential alternatives to Teflon filters, typically used for⁴⁴ capturing fine dust particles (PM_{2.5} and PM₁₀) from industrial flue gases. Experiments in our laboratory have also shown that such nanocellulose sheets possess very low porosity,²³ thus aiding in the effective trapping of dust particles.

Teflon-based sheets for dust capture applications have been well studied in the literature.^{45,46} Park *et al.* were able to maintain a

filtering efficiency above 80% after 225 min of filtration by optimizing the geometry of pleated (Teflon/glass) composite filters.³⁷ Dzubay and Barbour employed a coating of mineral oil on Teflon filters to achieve better adhesion of coarse dust particles to the filter medium.⁴⁰ Feng *et al.* showed that MnOx wrapped Teflon membranes were capable of removing ultrafine dust (less than 0.5 µm in diameter) due to their reduced pore size.⁴¹

Table 3 shows the gravimetric analysis of SMC refined nanocellulose sheets before and after PM_{2.5} capture. Here, LVB sheets were not considered because of the dense network of fibres, as well as the low aspect ratio of the fibres. Refining using 0.01 clearance produced nanocellulose fibers, as stated earlier, which led to better mechanical interlocking ability between fibers, thereby producing sheets with lower porosity (Fig. 14a). Lower porosity in SMC_0.01 sheets was also confirmed by previous

experiments in our lab,²³ which showed that longer time was required for air to traverse the sheet's thickness when compared to LVB sheets. This reduced porosity resulted in better PM_{2.5} capture of SMC_0.01 sheet (increase of 7%). In

the case of SMC_0.1 sheets, the dust capturing efficiency was found to decrease 10-fold (weight increase of 0.7% only), compared to SMC_0.01 sheets, due to high porosity, as seen in Figure 14b.

Table 3
Gravimetric analysis of SMC sheets subjected to dust capture test

Sheet	Initial weight (g)	Final weight (g)	Weight increase (%)
SMC-0.1	0.4163	0.4193	0.72
SMC-0.01	0.4160	0.4470	7.45

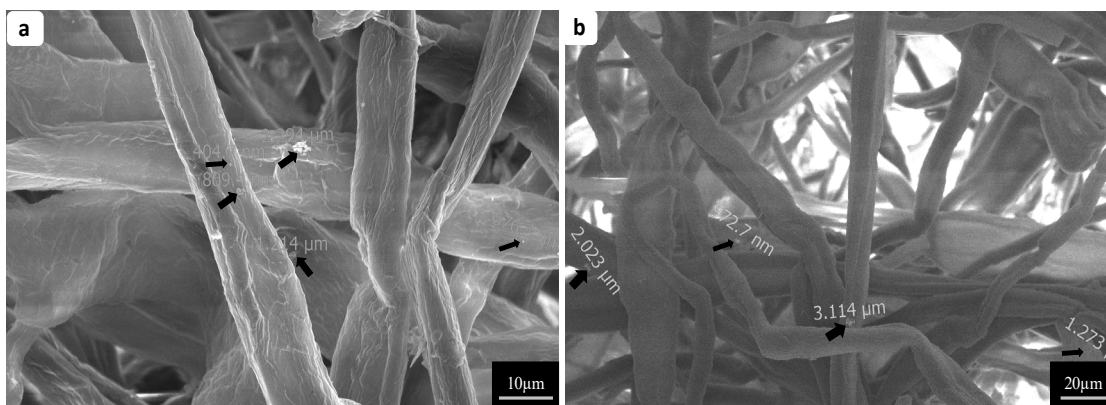


Figure 14: (a) Micrographs of SMC_0.01 sheet and (b) of SMC_0.1 sheet after dust capture; black arrows indicate PM_{2.5} dust particles, except one particle of 3.1 μm

CONCLUSION

In this study, processing of micro- and nanocellulose fibres and their characterization were carried out using microscopy, TGA and tensile testing. Although both refining techniques were able to decrease the diameter of pulp fibres, nanocellulose fibres were obtained only after refining using the Super Masscolloider (SMC). A greater decrease in length was found when fibres were refined using the Lab Valley Beater (LVB), whereas the SMC refining was able to retain almost 75% of the original length (approx. 1200 μm). The sheets made from LVB refined microcellulose fibres (by evaporating the water) revealed approx. 28-45 MPa of tensile strength due to the large number of fines and “surface fibrillation”, resulting in greater mechanical interlocking between fibres. The sheets made from SMC refined micro- and nanocellulose fibres (by evaporating the water) revealed 0.05-2.8 MPa of tensile strength due to the lower number of fines and lack of surface fibrillation, indicating the low impact of fibre aspect ratio, when compared to the number of fines. Increased refining time or intensity also led to an increase in

tensile strength of the sheet prepared from LVB or SMC refined fibres, possibly due to the increase in fines content. Therefore, for packing applications, pulp fibres refined with LVB can be employed due to their superior mechanical properties. Nanocellulose fibre based sheets obtained from SMC refining (high surface area and controlled porosity) can be used to retain a huge amount of dust, which can recommend them for PM_{2.5} dust capture application even at higher temperatures (around 60 °C) and longer durations (40 days). The current study revealed 10-fold higher capturing efficiency for SMC_0.01 sheets, compared to SMC_0.1 sheets, when tested against PM_{2.5} dust particles. TGA analysis revealed slightly better thermal stability for SMC refined fibres (till 250 °C) due to the loose network of micro/nano cellulose sheets. It is highly recommended to use blends of LVB and SMC refined pulp fibres to make industrial filters with high surface area and better mechanical (~25 MPa) and thermal properties (>250 °C).

ACKNOWLEDGEMENTS: The authors would like to thank Mr. Suresh and other members of

CAL Lab for SEM and TGA analyses of micro- and nanocellulose fibres. Help received from Mr. Khan, Mr. Appalareddy, and Mr. Lokesh (Pharmacy) in tensile testing, and from Mr. Bhaskar Raju and Mr. Hemanth in microscopy experiments and dust capture analysis is highly appreciated. We would also like to thank Mr. Murali and Mr. Bhaskar Reddy from Central workshop for their co-operation in making samples.

REFERENCES

- ¹ S. H. Osong, S. Norgen and P. Engstrand, *Cellulose*, **23**, 93 (2016), <https://doi.org/10.1007/s10570-015-0798-5>
- ² M. Pydimalla, N. S. Reddy and R. B. Adusumalli, *Cellulose Chem. Technol.*, **53**, 479 (2019), <https://doi.org/10.35812/CelluloseChemTechnol.2019.53.48>
- ³ R. B. Adusumalli, R. Raghavan, R. Ghisleni, T. Zimmermann and J. Michler, *Appl. Phys. A*, **100**, 447 (2010), <https://doi.org/10.1007/s00339-010-5847-1>
- ⁴ R. B. Adusumalli, W. M. Mook, R. Passas, P. Schwaller and J. Michler, *J. Mater. Sci.*, **45**, 2558 (2010), <https://doi.org/10.1007/s10853-010-4226-9>
- ⁵ S. Bauer and A. B. Ibanez, *Biotechnol. Bioeng.*, **11**, 2355 (2014), <https://doi.org/10.1002/bit.25276>
- ⁶ C. Salas, T. Nypelo, C. Rodriguez-Abreu, C. Carrillo and O. J. Rojas, *Curr. Opin. Colloid Interface Sci.*, **19**, 383 (2014), <https://doi.org/10.1016/j.cocis.2014.10.003>
- ⁷ N. Amirallian, P. K. Annamalai, P. Memmott and D. J. Martin, *Cellulose*, **22**, 2483 (2015), <https://doi.org/10.1007/s10570-015-0688-x>
- ⁸ Y. Xiao, Y. Liu, X. Wang, M. Li, H. Lei *et al.*, *Int. J. Biol. Macromol.*, **140**, 225 (2019), <https://doi.org/10.1016/j.ijbiomac.2019.08.160>
- ⁹ W. Chen, H. Yu, Y. Liu, P. Chen, M. Zhang *et al.*, *Carbohydr. Polym.*, **83**, 1804 (2011), <https://doi.org/10.1016/j.carbpol.2010.10.040>
- ¹⁰ X. Chen, E. Kuhn, W. Wang, S. Park, K. Flanagan *et al.*, *Bioresour. Technol.*, **147**, 401 (2013), <https://doi.org/10.1016/j.biortech.2013.07.109>
- ¹¹ S. Varanasi, L. Henzel, S. Sharman, W. Batchelor and G. Garnier, *Carbohydr. Polym.*, **184**, 307 (2018), <https://doi.org/10.1016/j.carbpol.2017.12.056>
- ¹² V. Leung and F. Ko, *Polym. Adv. Technol.*, **22**, 350 (2011), <https://doi.org/10.1002/pat.1813>
- ¹³ Q. Q. Wang, J. Y. Zhu, R. Gleisner, T. A. Kuster, U. Baxa *et al.*, *Cellulose*, **19**, 1631 (2012), <https://doi.org/10.1007/s10570-012-9745-x>
- ¹⁴ H. R. Motamedian, A. E. Halilovic and A. Kulachenko, *Cellulose*, **26**, 4099 (2019), <https://doi.org/10.1007/s10570-019-02349-5>
- ¹⁵ H. P. S. Abdul Khalil, Y. Davoudpour, M. N. Islam, A. Mustapha, K. Sudesh *et al.*, *Carbohydr. Polym.*, **99**, 649 (2014), <https://doi.org/10.1016/j.carbpol.2013.08.069>
- ¹⁶ D. Bandera, J. Sapkota, S. Josset, C. Weder, P. Tingaut *et al.*, *React. Funct. Polym.*, **85**, 134 (2014), <https://doi.org/10.1016/j.reactfunctpolym.2014.09.009>
- ¹⁷ G. A. Smook, "Handbook for Pulp and Paper Technologists", 4th ed., Vancouver, Angus Wilde Publications Inc., 1992, pp. 194-204, <https://trove.nla.gov.au/work/22361628?q&versionId=34741612>
- ¹⁸ M. Pydimalla and R. B. Adusumalli, *Nord. Pulp Pap. Res. J.*, **35**, 161 (2019), <https://doi.org/10.1515/npprj-2019-0055>
- ¹⁹ N. Rambabu, S. Panthapulakkal, M. Sain and A. K. Dalai, *Ind. Crop. Prod.*, **83**, 746 (2016), <https://doi.org/10.1016/j.indcrop.2015.11.083>
- ²⁰ M. L. Hassan, A. P. Mathew, E. A. Hassan, N. A. El-Wakil and K. Oksman, *Wood Sci. Technol.*, **46**, 193 (2012)
- ²¹ T. E. Motaung and T. H. Mokhothu, *Fiber. Polym.*, **3**, 343 (2016), <https://doi.org/10.1007/s12221-016-5430-2>
- ²² M. Pydimalla, B. R. Muthyala and R. B. Adusumalli, *Sugar Tech.*, **21**, 1003 (2019), <https://doi.org/10.1007/s12355-019-00719-8>
- ²³ P. Gulipalli, S. Borle, K. Chivukula and R. B. Adusumalli, *Mater. Today Proc.*, **72**, 402 (2022), <https://doi.org/10.1016/j.matpr.2022.08.189>
- ²⁴ I. Sahoo, C. Kaushik, M. Pydimalla and R. B. Adusumalli, *IPPTA*, **31**, 112 (2019), [E2-2019-Paper10.pdf \(ippta.co\)](https://doi.org/10.1007/s12221-019-00719-8)
- ²⁵ K. L. Spence, R. A. Venditti, O. J. Rojas, Y. Habibi and J. J. Pawlak, *Cellulose*, **18**, 1097 (2011), <https://doi.org/10.1007/s10570-011-9533-z>
- ²⁶ L. V. Haule, C. M. Carr and M. Rigout, *J. Clean. Prod.*, **112**, 4445 (2016), <https://doi.org/10.1016/j.jclepro.2015.08.086>
- ²⁷ J. Zeng, F. Hu, Z. Cheng, B. Wang and K. Chen, *Cellulose*, **28**, 3389 (2021), <https://doi.org/10.1007/s10570-021-03702-3>
- ²⁸ V. Kumar, P. Pathak and N. K. Bhardwaj, *Appl. Nanosci.*, **11**, 101 (2021), <https://doi.org/10.1007/s13204-020-01575-9>
- ²⁹ H. Yousefi, M. Faezipour, T. Nishino, A. Shakeri and G. Ebrahimi, *Polym. J.*, **43**, 559 (2011), <https://doi.org/10.1038/pj.2011.31>
- ³⁰ H. Yousefi, M. Faezipour, S. Hedjazi, M. M. Mousavi, Y. Azusa *et al.*, *Ind. Crop. Prod.*, **43**, 732 (2013), <https://doi.org/10.1016/j.indcrop.2012.08.030>
- ³¹ K. Abe, S. Iwamoto and H. Yano, *Biomacromolecules*, **8**, 3276 (2007), <https://doi.org/10.1021/bm700624p>
- ³² N. Lavoine, I. Desloges, A. Dufresne and J. Bras, *Carbohydr. Polym.*, **90**, 735 (2012), <https://doi.org/10.1016/j.carbpol.2012.05.026>
- ³³ A. B. Vanzetto, L. V. R. Beltrami and A. J. Zattera, *Cellulose*, **28**, 6967 (2021), <https://doi.org/10.1007/s10570-021-03982-9>
- ³⁴ J. Wu, R. Chandra and J. Saddler, *Sustain. Energ. Fuels*, **3**, 227 (2019), <https://doi.org/10.1039/C8SE00452H>

- ³⁵ F. J. Kilzer and A. Broido, *Pyrodynamics*, **2**, 151, (1965), <https://www.fs.usda.gov/research/treesearch/50136>
- ³⁶ W. Chen, H. Yu, Y. Liu, Y. Hai, M. Zhang *et al.*, *Cellulose*, **18**, 433 (2011), <https://doi.org/10.1007/s10570-011-9497-z>
- ³⁷ B. H. Park, M.-H. Lee, Y. M. Jo and S. B. Kim, *J. Air Waste Manag. Assoc.*, **62**, 1257 (2012), <https://doi.org/10.1080/10962247.2012.696530>
- ³⁸ H. J. Yoon, D. H. Kim, W. Seung, U. Khan, T. Y. Kim *et al.*, *Nano Energ.*, **63**, 103857 (2019), <https://doi.org/10.1016/j.nanoen.2019.103857>
- ³⁹ C. A. Lawrence and P. Liu, *Chem. Eng. Technol.*, **29**, 957 (2006), <https://doi.org/10.1002/ceat.200600055>
- ⁴⁰ T. G. Dzubay and R. K. Barbour, *J. Air Pollut. Contr. Assoc.*, **33**, 692 (1983)
- ⁴¹ S. Feng, M. Zhou, F. Han, Z. Zhong and W. Xing, *Chin. J. Chem. Eng.*, **28**, 1260 (2020), <https://doi.org/10.1016/j.cjche.2019.11.014>
- ⁴² P. Gulipalli, V. Viswanathan, C. Babu and M. R. Adusumalli, *IPPTA*, **35**, 149 (2023), <https://ippta.co/wp-content/uploads/2023/03/149-155.pdf>
- ⁴³ Z. Xiong, J. Lin, X. Li, F. Bian and J. Wang, *ACS Appl. Mater. Interfaces*, **13**, 12408 (2021), <https://doi.org/10.1021/acsami.1c01286>
- ⁴⁴ S. Ahn, E. Shim, Y. Kim, Y.-S. Bae and H. Eom, *Process Saf. Environ. Prot.*, **162**, 914 (2022), <https://doi.org/10.1016/j.psep.2022.04.067>
- ⁴⁵ X. Li, X.-X. Wang, T.-T. Yue, Y. Xu, M.-L. Zhao *et al.*, *Polymers*, **11**, 590 (2019), <https://doi.org/10.3390/polym11040590>
- ⁴⁶ M. Cho, V. Hiremath and J. G. Seo, *Atmos. Environ.: X*, **12**, 100138 (2021), <https://doi.org/10.1016/j.aeaoa.2021.100138>